Cross sections for ^{238}U$(n,n'\gamma)$ and ^{238}U$(n,2n\gamma)$ reactions at incident neutron energies between 5 and 14 MeV

A. Hutcheson,[1,5,*] C. Angell,[3,5] J. A. Becker,[7] A. S. Crowell,[1,5] D. Dashdorj,[2,7] B. Fallin,[1,5] N. Fotiades,[6] C. R. Howell,[1,5]
H. J. Karwowski,[3,5] T. Kawano,[6] J. H. Kelley,[2,5] E. Kwan,[1,5] R. A. Macri,[7] R. O. Nelson,[6]
R. S. Pedroni,[4,5] A. P. Tonchev,[1,5] and W. Tornow[1,5]

[1]*Department of Physics, Duke University, Durham, North Carolina 27708, USA*
[2]*North Carolina State University, Raleigh, North Carolina 27695, USA*
[3]*Department of Physics and Astronomy, University of North Carolina, Chapel Hill, North Carolina 27599, USA*
[4]*North Carolina A&T State University, Greensboro, North Carolina 27411, USA*
[5]*Triangle Universities Nuclear Laboratory, Durham, North Carolina 27708, USA*
[6]*Los Alamos National Laboratory, Los Alamos, New Mexico 87545, USA*
[7]*Lawrence Livermore National Laboratory, Livermore, California 94551, USA*

Precision measurements of ^{238}U$(n,n'\gamma)$ and ^{238}U$(n,2n\gamma)$ partial cross sections have been performed at Triangle Universities Nuclear Laboratory (TUNL) to improve crucial data needed for testing nuclear reaction models in the actinide mass region. A pulsed and monoenergetic neutron beam was used in combination with high-resolution γ-ray spectroscopy to obtain partial cross sections for incident neutron energies between 5 and 14 MeV. γ-ray yields were measured with high-purity germanium clover and planar detectors. Measured partial cross-section data are compared with previous results using white and monoenergetic neutron beams and calculations from the GNASH and TALYS Hauser-Feshbach statistical-model codes. Present experimental results are in fair to good agreement with most of the existing data for the ^{238}U$(n,n'\gamma)$ reaction. However, significant discrepancies are observed for the ^{238}U$(n,2n\gamma)$ reaction.

PACS number(s): 21.10.−k, 25.40.Fq, 27.90.+b, 28.20.−v

I. INTRODUCTION

Neutron-induced reactions on uranium isotopes in the energy range below 15 MeV are of fundamental importance in the field of nuclear energy and nuclear transmutation [1]. For example, these interactions dominate neutron generation and neutron transport in accelerator supported nuclear reactors, such as the proposed accelerator driven system of Ref. [2]. In addition, since inelastic neutron scattering cross-section data provide unique information on decay mechanisms of highly excited nuclei, their comparison with theoretical model calculations can yield valuable information about nuclear structure and the reaction mechanism of these processes. Furthermore, accurate modeling of the reaction mechanism is important for designing the next generation of nuclear reactors.

Direct measurements of inelastic scattering cross sections for uranium are difficult at best. Neutron counting experiments suffer from large backgrounds due to fast neutrons produced in neutron-induced fission. In addition, the time-of-light technique is hampered by the very close level spacings in this actinide nucleus, which are difficult to resolve by direct neutron detection. Therefore, following Ref. [3], an indirect technique involving high-resolution γ-ray spectroscopy was used to deduce reaction cross-section information from measurements of neutron-induced γ-ray spectra. The measured partial γ-ray cross-section data can be compared with nuclear model calculations, including Hauser-Feshbach theory, which

allow inference of channel cross-section results. Daughter nuclei from inelastic scattering reactions are typically left in an excited state that decays by prompt γ-ray emission. Transitions to low-lying states typically account for the majority of decays and therefore can be used to reliably estimate reaction cross sections. Measurements performed by previous groups, however, have produced discrepant data. For some transitions, e.g., the 1060.3 keV ($2^+ \rightarrow 0^+$) transition in ^{238}U, the cross-section data differ by as much as a factor of 2 from data measured by Fotiades *et al.* [4], Olsen *et al.* [5], and Voss *et al.* [6].

High-resolution γ-ray spectra have been measured for the ^{238}U$(n,n'\gamma)^{238}$U and ^{238}U$(n,2n\gamma)^{237}$U reactions at Triangle Universities Nuclear Laboratory (TUNL) using high-purity germanium detectors in combination with pulsed, quasimonoenergetic neutron beams. Excitation functions of observed γ-ray transitions in ^{238}U and ^{237}U were derived for incident neutron energies between 5 and 14 MeV. Our measurements are part of a larger experimental effort aimed at studying the systematics of $(n,xn\gamma)$ reaction cross sections using monoenergetic neutron beams to complement and to compare against existing data obtained with continuous energy (white) neutron beams. This paper focuses on the detailed presentation of our experimental results and their comparison with model calculations and earlier measurements.

II. EXPERIMENTAL SETUP

In this experiment, ^{238}U$(n,xn\gamma)$ partial cross-section data were measured. The uranium target was irradiated with pulsed,

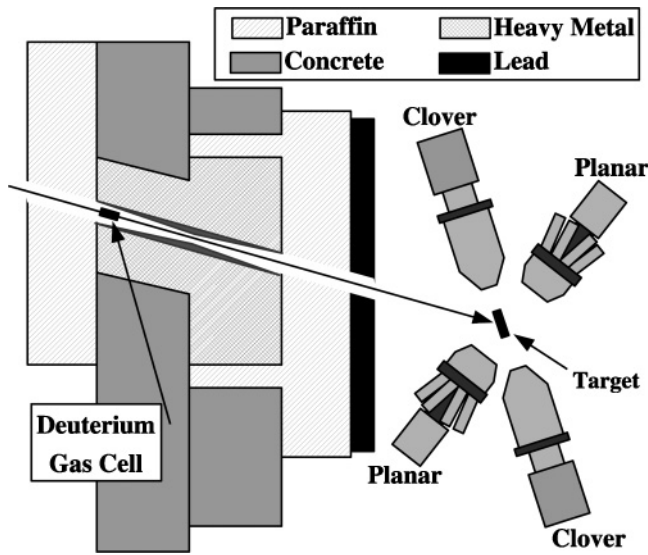*hutch@tunl.duke.edu; Present address: U.S. Naval Research Laboratory, Washington, DC 20375.

FIG. 1. Shielded neutron source area at TUNL.

nearly monoenergetic neutrons, and a combination of high-purity germanium (HPGe) clover and planar detectors was used to measure the emitted γ rays from the excited nucleus. In-beam measurements were performed in the shielded neutron source area at TUNL shown in Fig. 1.

Simultaneous irradiation of a natural iron foil and measurement of the emitted γ rays enabled relative cross-section normalization. The measurements were performed over a span of four years and represent about 550 hr of beam time.

Fast neutrons used in this experiment were produced via the $^2\mathrm{H}(d,n)^3\mathrm{He}$ reaction by bombarding a deuterium gas cell with an accelerated beam of deuterons. The deuteron beam utilized in the source reaction was produced by a duoplasmatron ion source located in the low-energy end of the TUNL accelerator bay. A continuous beam of ions was extracted from the source head which was held at -50 kV with respect to ground. After extraction, the ion beam was pulsed using a combination of two electrostatic choppers and a single double-drift buncher [7]. This system, in combination with the ion source, can provide up to 3 μA of pulsed deuteron current with a pulse width of 2 ns and a repetition rate of 2.5 MHz or smaller (by factors of 2). After being properly pulsed, the deuteron beam was accelerated by way of the model FN Tandem Van de Graaff accelerator before bombarding a cylindrical gas cell pressurized to 7.8 atm with 99.999% pure deuterium gas. Deuteron ions entered the cell through a 6.35 μm Havar foil, which separated the deuterium gas from the vacuum of the beamline. The downstream end of the gas cell was capped by a 0.05 cm thick gold beam stop. The gas cell was a 3 cm long copper cylinder with a diameter of 1 cm. The cell was cooled by 10°C distilled water circulated through copper coils wrapped around the cell as well as by two compressed air jets directed at either end of the cell.

The $^2\mathrm{H}(d,n)^3\mathrm{He}$ reaction has a very large cross section for the production of forward-angle neutrons at energies between 7 and 20 MeV [8]. The most energetic neutrons produced by this reaction are emitted at forward angles with both the neutron energy and cross section for production rapidly

diminishing as the angle is increased from 0°. The target area was shielded from background radiation produced at the gas cell by a multilayered wall composed of concrete, paraffin, lead, copper, and iron. A double-truncated collimator, 117 cm long and made from tapered copper (79 cm long) and polyethylene bars (38 cm long), was fitted inside an opening in the shielding wall with the throat 33.5 cm from the center of the gas cell. This collimator was designed to minimize the amount of neutrons scattered from the sides of the collimator wall, while allowing the uranium-iron target to be exposed to a spatially homogenous field of unscattered neutrons.

The target used for this experiment consisted of a 6.86 g rectangular $^{238}\mathrm{U}$ foil ($3.65 \times 5.20 \times 0.02$ cm) backed by rectangular foils of 99.5% natural iron foils of thickness 0.0038 cm and positioned in the neutron beam 215 cm downstream from the gas cell (74.5 cm from the shielding wall). γ rays emitted from the target were measured using a set of clover and planer HPGe detectors, each equipped with a bismuth germinate (BGO) suppression shield and NaI nose cone. The detectors were mounted on movable stands that rotated about the target position in the horizontal plane and allowed measurements at laboratory angles ranging from 0° to 140°. Additionally, the stands could move radially, allowing the front face of the detector to be positioned between 0 and 26 cm from the target.

This experiment utilized the Spectrodaq/SpecTCL data-acquisition program developed at the National Superconducting Cyclotron Laboratory at Michigan State University [9]. Real-time events were read into event files that were saved to disk, enabling offline analysis at a later time. In addition, real-time one- and two-dimensional histograms of incoming data could be viewed during data acquisition. Data-acquisition system dead times were measured using scalers and found to be $\sim$10–15%.

III. ANALYSIS

Data obtained from SpecTCL were histogrammed in 2×2 matrices of energy versus time-of-flight spectra for each detector in ASCII format. These matrices were then converted to line compressed format and analyzed using the Tv spectra- and matrix-analysis program [10]. Typical γ-ray spectra produced in these measurements contained hundreds of full-energy peaks resulting from natural background radiation, neutron-induced reactions in detector and shielding materials, and natural decay of the uranium targets, as well as from the prompt neutron-induced reactions of interest in the target.

Neutron time-of-flight spectra were generated by a time-to-digital converter (TDC) where the start signal was provided by an event in the Ge detector, while the stop signal came from a delayed signal from a capacitive pickoff unit located just before the deuterium gas cell. Events not time-correlated with neutron beam pulses appear as a flat background in the time spectrum. Beam-correlated events appear as prompt peaks above the flat background with the full width at half maximum (FWHM) dominated by the timing resolution of the detector ($\sim$10 ns for germanium detectors). An example time-of-flight spectrum for clover data is shown in Fig. 2.
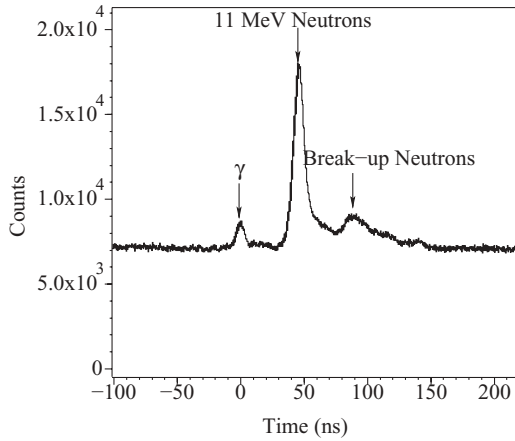
FIG. 2. Time-of-flight spectrum with clover detector for 11 MeV neutrons. Time is relative to γ-ray peak.

TABLE I. Partial list of identified peaks stemming from neutron-induced reactions in detector and shielding materials.

E_γ (keV)	Reaction	E_γ (keV)	Reaction
538.41	^{209}Bi$(n,2n)^{208}$Bi	886.40	^{209}Bi$(n,2n)^{208}$Bi
562.93	^{76}Ge$(n,n')^{76}$Ge	894.26	^{72}Ge$(n,n')^{72}$Ge
565.23	^{209}Bi$(n,2n)^{208}$Bi	896.00	^{209}Bi$(n,2n)^{208}$Bi
569.70	^{207}Pb$(n,n')^{207}$Pb	984.64	^{27}Al$(n,p)^{27}$Mg
595.85	^{74}Ge$(n,n')^{74}$Ge	1006.23	^{209}Bi$(n,2n)^{208}$Bi
601.49	^{209}Bi$(n,2n)^{208}$Bi	1014.42	^{27}Al$(n,n')^{27}$Al
650.60	^{209}Bi$(n,2n)^{208}$Bi	1033.31	^{209}Bi$(n,2n)^{208}$Bi
718.35	^{10}B$(n,n')^{10}$B	1039.49	^{70}Ge$(n,n')^{70}$Ge
803.06	^{206}Pb$(n,n')^{206}$Pb	1094.90	^{209}Bi$(n,2n)^{208}$Bi
823.25	^{209}Bi$(n,2n)^{208}$Bi	1204.21	^{74}Ge$(n,n')^{74}$Ge
834.01	^{72}Ge$(n,n')^{72}$Ge	1609.10	^{209}Bi$(n,2n)^{208}$Bi
843.74	^{27}Al$(n,n')^{27}$Al	1697.94	^{27}Al$(n,p)^{27}$Mg
867.90	^{74}Ge$(n,n')^{74}$Ge	1778.85	^{27}Al$(n,p\beta^-)^{28}$Si
874.41	^{27}Al$(n,\alpha)^{24}$Na	1808.66	^{27}Al$(n,d)^{26}$Mg

Timing gates were placed in the time-of-flight spectra around the monoenergetic neutron peak and, separately, around an equal number of channels in the flat accidental background area before the γ-ray peak (where no beam-correlated events can take place) to produce "prompt" and "accidental" γ-ray spectra, which could be subtracted to produce gated spectra associated with the neutron beam pulse.

However, because of the short flight path between the detectors and target (typically $\sim$10–15 cm) and the limited time resolution of the germanium detectors, time-of-flight techniques were unable to distinguish between γ rays emitted from the target and γ rays induced by fast neutrons scattering off the uranium target into detector or shielding materials surrounding the detectors. Therefore, special care was taken to identify these detector- and shielding-associated events. Spectra were collected in "empty target" runs where the beam was on but no target was present. Observed full-energy peaks were compared with the accepted energies of γ rays emitted from materials known to be present in the detectors and shields (^{70,72,74}Ge, ^{209}Bi, ^{27}Al, etc.). Because of the absence of uranium scatterer, neutron fluxes into the detector were considerably lower, resulting only from neutrons scattering from air or escaping through imperfections in the shielding wall. A partial list of identified peaks resulting from reactions in the detector and shielding materials is given in Table I.

Once target-related γ-ray peaks were properly identified and yields obtained, partial cross-section values were extracted. The angle-integrated partial cross section is given by

$$\sigma(E_\gamma) = N_\gamma(E_\gamma, \theta) \frac{(1 + \alpha)C_{\text{att}}}{\epsilon N_{\text{target}} \Phi t C_{\text{dead}} W(\theta)}, \qquad (1)$$

where $N_\gamma(E_\gamma, \theta)$ is the peak yield for a γ ray with energy E_γ in a detector positioned at angle θ, α is the internal conversion coefficient, C_{att} is a correction factor accounting for attenuation of the γ ray in the target, $W(\theta)$ is the angular distribution of γ-ray emission, ϵ is the absolute efficiency of the detector, N_{target} is the number of target atoms, t is the time of measurement, C_{dead} is the dead-time correction factor, and Φ is the neutron flux. Internal conversion coefficients were obtained from the BrIcc internal conversion coefficient database [11].

Absolute efficiencies for clover and planar detectors were measured offline using γ-ray standard calibration sources of about 1 μCi strength with peaks of well-known energy, and simulated using the MCNPX Monte-Carlo radiation transport code [12] to correct for finite geometry effects. Cross-section values were corrected for attenuation of γ rays in the target material using MCNPX simulations. As the number of detectors used in these measurements was limited, angular distributions could not be accurately obtained simply by fitting the data. Instead, angular distributions were calculated by combining theoretical framework [13] with spin-state orientation parameters obtained from the AVALANCHE code [14]. Neutron flux was determined from the measured yields for the 846.77 keV γ ray stemming from the $2^+ \rightarrow 0^+$ transition in ^{56}Fe. Angle-integrated ^{56}Fe$(n,n'\gamma)$ partial cross-section values for each incident neutron energy were obtained from the data measured by Nelson *et al.* [15].

IV. MODEL CALCULATIONS

Predicted partial cross-section data for ^{238}U$(n,n'\gamma)$ and ^{238}U$(n,2n\gamma)$ reactions were calculated using the statistical Hauser-Feshbach model as implemented in the GNASH [16] and TALYS [17] reaction codes. The general prescription for both of these codes is to assume reactions occur in a series of binary reactions where, for each step in the reaction chain, particle and γ-ray emission is calculated. For both calculations, direct reaction and transmission-coefficient calculations were obtained via the ECIS coupled-channels code [18]; this was done externally for GNASH but is implemented as a subroutine for TALYS. Preequilibrium effects are taken into account by both codes by using the semiclassical exciton model; however, spin-transfer effects, which are not taken into account in the exciton model, have been shown to be important to accurately calculate partial cross sections [19]. Therefore, in addition to a standard GNASH calculation, a second calculation (referred to as GNASH-FKK in this work) was
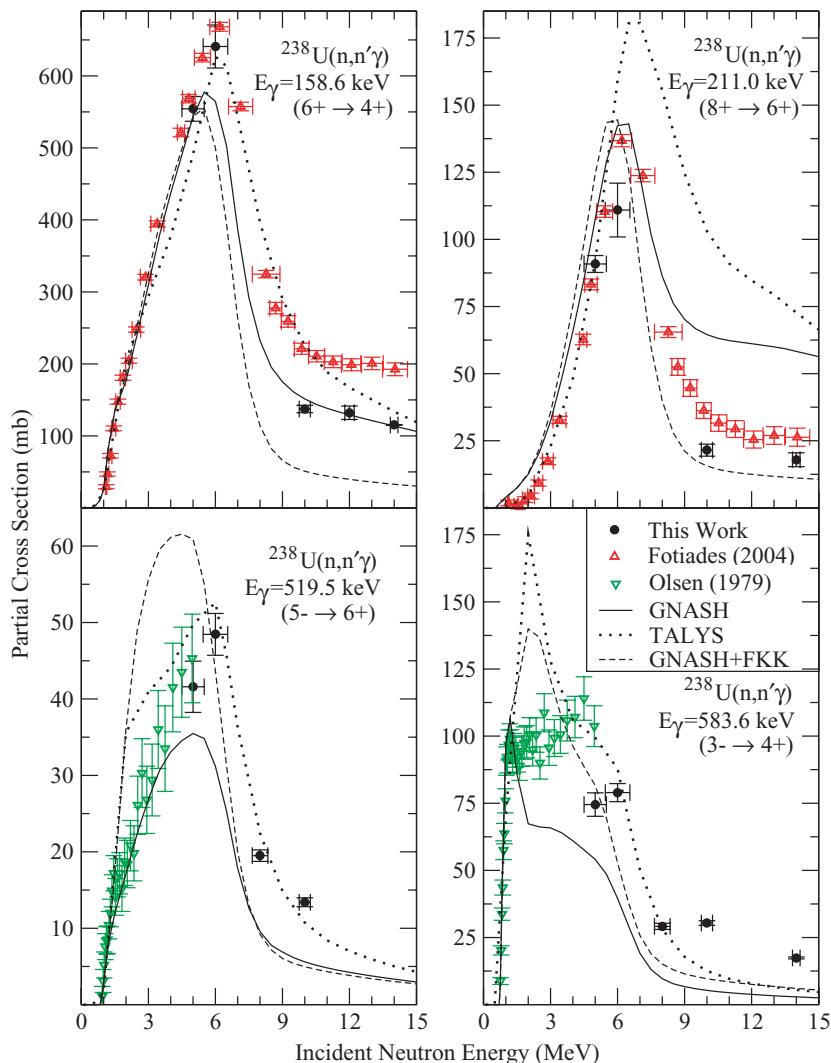
FIG. 3. (Color online) ^{238}U$(n,n'\gamma)$ partial cross-section data. Comparison with existing cross-section data from Fotiades *et al.* [4] and Olsen *et al.* [5] as well as GNASH and TALYS model calculations (see legend). Error bars reflect statistical uncertainties only.

performed where spin-distribution effects for multistep direct preequilbrium reactions were calculated externally using the theory of Feshbach, Kerman, and Koonin [20] and included in the GNASH calculation [21]. Input files for GNASH were tuned to previous measurements; TALYS input files used default values for all parameters with the exception of barrier height and width which were taken from the Reference Input Parameter Library (RIPL).

V. RESULTS AND DISCUSSION

Partial γ-ray cross-section values for nine transitions were observed for ^{238}U: seven ^{238}U$(n,n'\gamma)$ and two ^{238}U$(n,2n\gamma)$ transitions. These transitions had no beam-correlated or sample-correlated background interference of significance. Additional transitions were observed, but cross-section results were not extracted because of the inability to resolve the peaks of interest in the spectra caused by interference from peaks stemming from transitions in the detector material or interference from large background peaks resulting in poor statistics after subtraction. Results are shown and compared with published data in Fig. 3– 5. Error bars in this work reflect

statistical uncertainties only; systematic uncertainties for the partial cross-section measurements are given in Table II. Total systematic uncertainties are calculated by

$$\frac{\Delta\sigma}{\sigma} = \sqrt{\left(\frac{\Delta\Phi}{\Phi}\right)^2 + \left(\frac{\Delta\alpha}{\alpha}\right)^2 + \left(\frac{\Delta\epsilon}{\epsilon}\right)^2 + \left(\frac{\Delta m}{m}\right)^2}, \quad (2)$$

where Φ is the neutron flux, α is the internal conversion coefficient of the measured transition, ϵ is the absolute

TABLE II. Systematic uncertainties in the determination of cross-section data.

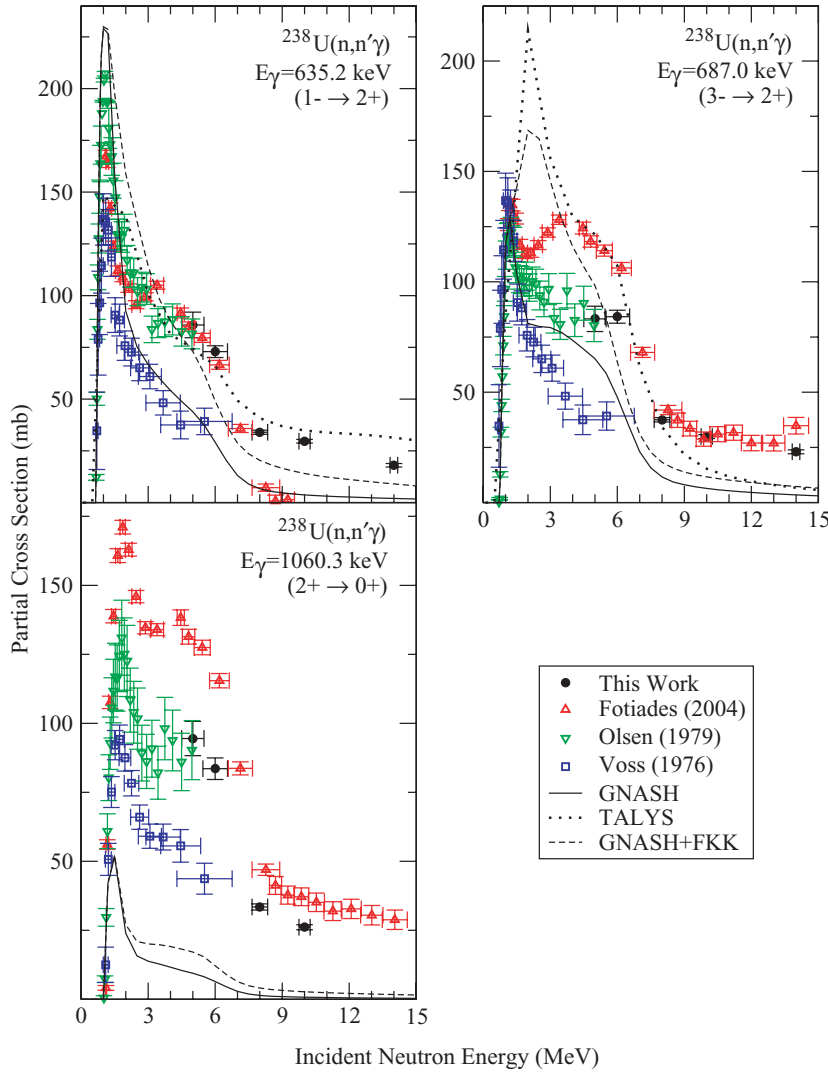| Value	^{238}U uncertainty
m_U	<1%
Φ	8.2%
α	1.4%
ϵ	2.2%
Total	8.6%

FIG. 4. (Color online) ^{238}U($n,n'\gamma$) partial cross-section data. Comparison with existing cross-section data from Fotiades *et al.* [4], Olsen *et al.* [5], and Voss *et al.* [6] as well as GNASH and TALYS model calculations. Error bars reflect statistical uncertainties only.

efficiency of the detector, and *m* is the mass of the uranium target.

A. ^{238}U($n,n'\gamma$)

In general, the cross sections measured in this work are in good agreement at lower energies with those measured by Fotiades *et al.* using the continuous energy (white) neutron beam from the spallation source at Los Alamos National Laboratory [4] as well as those measured by Olsen *et al.* [5]. However, for $E_n \geqslant 10$ MeV, our measured cross-section results for the 158.8 keV ($6^+ \rightarrow 4^+$) and 211.0 keV ($8^+ \rightarrow 6^+$) transitions (Fig. 3) are lower by $\sim$25% than those given by Fotiades *et al.* Additionally, our measured cross-section values deviate from those measured by Fotiades *et al.* at low energies for the 687.0 keV ($3^- \rightarrow 2^+$) and 1060.3 keV ($2^+ \rightarrow 0^+$) transitions and agree more closely with the data of Olsen *et al.* (Fig. 4). Model calculations are generally in agreement with measured cross-section data, though the FKK-corrected GNASH calculations generally reproduce measured values better than default exciton-model calculations. However, as

can be seen from Fig. 4, the model calculations are in clear disagreement with the experimental data for the $2^+ \rightarrow 0^+$ 1060.3 keV transition.

B. ^{238}U($n,2n\gamma$)

Cross-section data for the 121.2 keV ($\frac{11}{2}^+ \rightarrow \frac{7}{2}^+$) and 148.6 keV ($\frac{5}{2}^+ \rightarrow \frac{3}{2}^+$) transitions were determined for incident neutron energies of $E_n = 10$ and 14 MeV (see Fig. 5). Unlike those measured for ^{238}U($n,n'\gamma$)^{238}U, there is considerable disagreement between the cross-section data measured in this work and those given by Fotiades *et al.* Specifically, the Fotiades *et al.* data are larger by a factor of 3.5. The reason for this discrepancy is unknown; however, the Fotiades group's data are somewhat suspect because of the nearly 100 mb cross section measured below the ($n,2n$) reaction threshold ($E_n = 6.18$ MeV). GNASH calculations generally agree with the Fotiades group's data for the $\frac{5}{2}^+ \rightarrow \frac{3}{2}^+$ transition, while TALYS greatly overestimates the cross section, likely because of the incorrect preequilibrium spin distribution for this higher
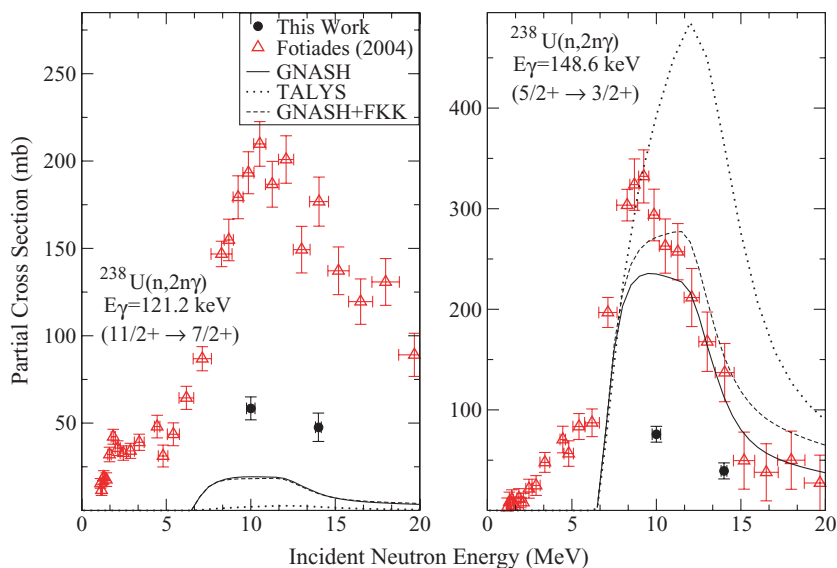
FIG. 5. (Color online) ^{238}U$(n,2n\gamma)$ cross-section data. Comparison with existing cross-section data from Fotiades *et al.* [4] as well as GNASH and TALYS model calculations. Error bars reflect statistical uncertainties only.

spin state. None of the calculations describe the $\frac{11}{2}^+ \to \frac{7}{2}^+$ transition.

VI. CONCLUSION

Neutron-induced partial γ-ray cross-section data have been measured for ^{238}U$(n,n'\gamma)^{238}$U and ^{238}U$(n,2n\gamma)^{237}$U using HPGe clover and planar detectors and a pulsed, monoenergetic neutron beam at Triangle Universities Nuclear Laboratory. Partial cross-section data were determined as a function of incident neutron energy for E_n between 5 and 14 MeV. Cross-section data were extracted from γ-ray yields, and corrections for detector efficiency, internal conversion, attenuation of the γ rays in the target, angular distribution, and dead-time were accounted for. Neutron flux was determined from the concurrent measurement of γ-ray yields from the 846.77 keV $(2^+ \to 0^+)$ transition in ^{56}Fe.

In total, cross-section data for 11 separate transitions were measured. Results are generally in fair to good agreement with existing data with the exception of the cross-section results for the two measured ^{238}U$(n,2n\gamma)^{237}$U transitions. Experimental data were compared with GNASH and TALYS model calculations and were generally found to be in reasonably good agreement, although large disagreements exist in some cases. Cross-section data for transitions from levels with relatively high spin, e.g., the 211.0 keV $(8^+ \to 6^+)$

transition in ^{238}U, clearly show the need for statistical models to incorporate the effect of multistep direct preequilibrium spin distributions to accurately calculate the cross sections for higher incident neutron energies. However, for medium-spin transitions, e.g., the 158.6 keV $(6^+ \to 4^+)$ transition in ^{238}U, the FKK corrections are inconsistent in reliably reproducing the measured cross-section data, which would indicate that more work is required in understanding lower-spin preequilibrium transitions. Further tuning of the statistical model codes is suggested to more accurately reproduce the measured cross-section data and to better predict the total reaction-channel cross section in regions where little or no data exist.

[1] R. C. Haight, M. B. Chadwick, and D. J. Vieira, Los Alamos Sci. Mag. No. 30, 52 (2006).

[2] G. Aliberti, G. Palmiotti, M. Salvatores, and C. Stenberg, Nucl. Sci. Eng. **146**, 13 (2004).

[3] L. Bernstein, J. Becker, P. Garrett, W. Younes, D. McNabb, D. Archer, C. McGrath, H. Chen, W. Ormand, M. Stoyer *et al.*, Phys. Rev. C **65**, 021601(R) (2002).

[4] N. Fotiades, G. D. Johns, R. O. Nelson, M. B. Chadwick, M. Devlin, M. S. Wilburn, P. G. Young, J. A. Becker, D. E. Archer, L. A. Bernstein *et al.*, Phys. Rev. C **69**, 024601 (2004).

[5] D. K. Olsen, G. L. Morgan, and J. W. McConnell, in *Proceedings of the International Conference on Nuclear Cross Sections for Technology: Knoxville, TN, 22–26 Oct. 1979*, edited by J. L. Fowler, C. H. Johnson, and C. D. Bowman (National Bureau of Standards, Washington, 1979), p. 677.

[6] F. Voss, S. Cierjacks, D. Erbe, and G. Schmatz, Kernforschungszentrum Karlsruhe Rep. No. 2379, 1976 (unpublished).

[7] S. Wender, C. Floyd, T. Clegg, and W. Wylie, Nucl. Instrum. Methods **174**, 341 (1980).

[8] M. Drosg, Nucl. Sci. Eng. **67**, 190 (1978).

[9] R. Fox, C. Bolen, K. Orji, and J. Venema, in 11th Annual Tcl/Tk Conference, New Orleans, Louisiana, October 11–15 2004, http://www.tcl.tk/community/tcl2004/Papers/.

[10] J. Theuerkauf, S. Esser, S. Krink, M. Luig, N. Nicolay, O. Stuch, and H. Wolters, *Program Tv* (Institute for Nuclear Physics, Cologne, 1993).

[11] T. Kibèdi, T. Burrows, M. Trzhaskovskaya, P. Davidson, and C. Nestor Jr., Nucl. Instrum. Methods Phys. Res. A **589**, 202 (2008).

[12] G. McKinney, J. Durkee, J. Hendricks, M. James, D. Pelowitz, L. Waters, and F. Gallmeier, in *Proceedings of the Hadronic Shower Simulation Workshop, Batavia, Illinois, 6–8 Sept. 2006*, edited by M. Albrow and R. Raja (American Institute of Physics, Melville, NY, 2007), p. 81.

[13] H. Olliver, T. Glasmacher, and A. E. Stuchbery, Phys. Rev. C **68**, 044312 (2003).

[14] P. Cejnar, S. Drissi, and J. Kern, Nucl. Phys. **A561**, 317 (1993).

[15] R. Nelson, N. Fotiades, M. Devlin, J. Becker, P. Garrett, and W. Younes, in *Proceedings of the International Conference on Nuclear Data for Science and Technology: Santa Fe, New Mexico, 26 Sept.–1 Oct. 2004*, edited by R. C. Haight (American Institute of Physics, Melville, NY, 2005), vol. 1, p. 838.

[16] P. Young, E. Arthur, and M. Chadwick, in *Nuclear Reaction Data and Nuclear Reactors: Physics, Design, and Safety: Proceedings of the Workshop: ICTP, Trieste, Italy, 23 Feb.–27 Mar. 1998*, edited by P. Oblonžinský and A. Gandini (World Scientific, Singapore, 1999), vol. 1, p. 227.

[17] A. Koning, S. Hilaire, and M. Dijvestijn, in *Proceedings of the International Conference on Nuclear Data for Science and Technology: Nice, France, 22–27 Apr. 2007*, edited by O. Bersillon, F. Gunsing, E. Bauge, R. Jacqmin, and S. Leray (EDP Sciences, Les Ulis, France, 2008).

[18] J. Raynal, in *Proceedings of the Specialists' Meeting on the Nucleon Nucleus Optical Model up to 200 MeV: Bruyères-le-Chatel, France, 13–15 Nov. 1996* (organization Nuclear Energy Agency, Issy-les-Moulineaux, France, 1997), p. 159.

[19] D. Dashdorj, T. Kawano, P. E. Garrett, J. A. Becker, U. Agvaanluvsan, L. A. Bernstein, M. B. Chadwick, M. Devlin, N. Fotiades, G. E. Mitchell *et al.*, Phys. Rev. C **75**, 054612 (2007).

[20] H. Feshbach, A. Kerman, and S. Koonin, Ann. Phys. (NY) **125**, 429 (1980).

[21] T. Kawano, T. Ohsawa, M. Baba, and T. Nakagawa, Phys. Rev. C **63**, 034601 (2001).